

Photon collider at TESLA

Valery Telnov

*Institute of Nuclear Physics, 630090 Novosibirsk, Russia
and DESY, Notkestr.85, D-22603 Hamburg, Germany*

Abstract

High energy photon colliders ($\gamma\gamma$, γe) based on backward Compton scattering of laser light is a very natural addition to e^+e^- linear colliders. In this report we consider this option for the TESLA project. Recent study has shown that the horizontal emittance in the TESLA damping ring can be further decreased by a factor of four. In this case the $\gamma\gamma$ luminosity in the high energy part of spectrum can reach $0.3\text{--}0.5 L_{e^+e^-}$. Typical cross sections of interesting processes in $\gamma\gamma$ collisions are higher than those in e^+e^- collisions by about one order of magnitude, so the number of events in $\gamma\gamma$ collisions will be more than in e^+e^- collisions. Photon colliders can, certainly, give additional information and they are the best for the study of many phenomena. The main question is now the technical feasibility. The key new element in photon colliders is a very powerful laser system. An external optical cavity is a promising approach for the TESLA project. A free electron laser is another option. However, a more straightforward solution is “an optical storage ring (optical trap)” with diode pumped laser injector which is today technically feasible. This paper briefly review the status of a photon collider based at TESLA, its possible parameters and existing problems.

PACS: 29.17.+w, 41.75.Ht, 41.75.Lx, 13.60.Fz

Key words: photon collider; linear collider; photon photon; gamma gamma; electron photon; photon electron; Compton scattering; backscattering

1 Introduction

Over the last decade, several laboratories in the world have been working on linear e^+e^- collider projects with an energy from several hundreds GeV up to several TeV: these are NLC(USA) [1], JLC(Japan) [2], TESLA(Europe) [3],

¹ e-mail: telnov@inp.nsk.su, check via e-mail current address.

CLIC (CERN) [4]. Beside e^+e^- collisions, linear colliders can “convert” electrons to high energy photons using the Compton backscattering of laser light, thus obtaining $\gamma\gamma$ and γe collisions with energies and luminosities close to those in e^+e^- collisions [5–10].

The basic scheme of a photon collider is shown in Fig. 1. Two electron beam after the final focus system travel towards the interaction point (IP) and at a distance b of about 0.1-0.5 cm from the IP collide with the focused laser beam. After scattering, the photons have an energy close to that of the initial electrons and follow their direction to the interaction point (IP) (with some small additional angular spread of the order of $1/\gamma$), where they collide with a similar counter moving high energy photon beam or with an electron beam. To avoid background from the disrupted beams hitting the final quads, a crab crossing scheme is used (fig.1b).

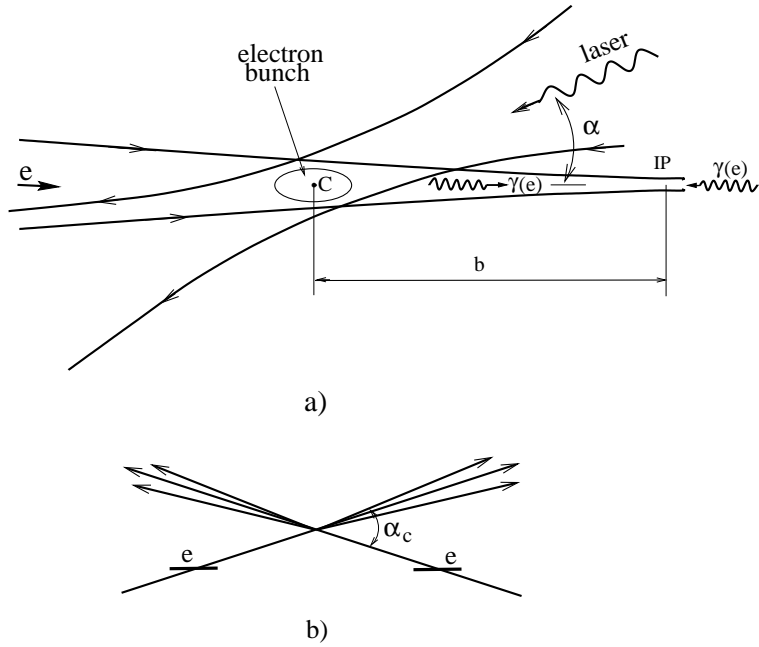


Fig. 1. Scheme of $\gamma\gamma$, γe collider.

The maximum energy of the scattered photons (in direction of electrons) is

$$\omega_m = \frac{x}{x+1} E_0; \quad x = \frac{4E_0 \omega_0 \cos^2 \alpha / 2}{m^2 c^4} \simeq 15.3 \left[\frac{E_0}{\text{TeV}} \right] \left[\frac{\omega_0}{\text{eV}} \right], \quad (1)$$

where E_0 is the electron energy, ω_0 the energy of the laser photon, α is the angle between electron and laser beam (see, fig.1a).

For example: $E_0 = 250$ GeV, $\omega_0 = 1.17$ eV ($\lambda = 1.06$ μm) (Nd:Glass and other powerful solid state lasers) $\Rightarrow x = 4.5$ and $\omega/E_0 = 0.82$.

The energy of the backscattered photons grows with increasing x . However, at $x > 4.8$ the high energy photons are lost due to e^+e^- creation in the collisions with laser photons [6,8,9]. The optimum laser wave length $\lambda[\mu\text{m}] \sim 4E[\text{TeV}]$. So, for $\gamma\gamma$ collisions the maximum energy is $z_m = W_{\gamma\gamma,max}/2E_0 = x/(x+1) \sim 0.8$ and in γe collisions $z_m = W_{\gamma e,max}/2E_0 = \sqrt{x/x+1} \sim 0.9$.

For an introduction to photon colliders see introductory talks at this Workshop [11],[12] and refs [6,8,9].

Below I will discuss most important issues connected with a photon collider based on the TESLA e^+e^- linear collider. TESLA is the superconducting linear collider on the c.m.s. energy $2E = 500$ GeV, with the possibility of upgrading up to 800 GeV. In comparison with other projects based on “normal” conducting structures TESLA has several advantages: higher RF efficiency and correspondingly higher possible luminosity; much larger distance between bunches which makes readout and background problems much easier. Larger aperture of the accelerating structure (and correspondingly smaller wake fields) allows bunches with very small emittances to be accelerated without emittance dilution. All this makes the TESLA project very attractive. Many European high-energy physicists consider TESLA as the next after LHC project. Now intensive work is going on both on accelerator, physics and detector with the intent to submit Technical Design Report (TDR) in Spring 2001.

Beside e^+e^- collisions in TESLA project a second interaction region for $\gamma\gamma$ and γe collision is foreseen [13]. It is very important to include in the basic design of the collider all that is necessary for a photon collider: special interaction region with the crab crossing, minimization of beam emittances and their preservation along the LC, space for lasers and laser optics, beam dump etc. This work is underway. Detector for $\gamma\gamma, \gamma e$ collisions may be very similar to that for e^+e^- collision, though with some complication connected with the focusing mirrors optics which should be placed inside the detector. The most important key element of the photon collider is a laser system with very unique parameters. Development of the laser system is currently the highest priority: “To be or not to be” for photon colliders will be determined by the success of this laser R&D.

Below I will briefly discuss the following essential topics:

- (1) physics motivation;
- (2) possible parameters of the photon collider at TESLA;
- (3) lasers, optics;
- (4) backgrounds and some other issues.

2 Physics

Physics motivation for photon colliders is a very important issue. The next linear e^+e^- collider should give some new information after LHC, photon colliders should give something new (or better accuracy) in addition to e^+e^- . In general, physics in e^+e^- and $\gamma\gamma$, γe collisions is quite similar because the same particles can be produced. However, it is always better to study new phenomena in various reactions because they give complementary information. Some phenomena can best be studied at photon colliders due to better accuracy or larger accessible masses.

The second aspect important for physics motivation is the luminosity. Typical luminosity distribution in $\gamma\gamma$ and γe collisions has a high energy peak and some low energy part (see the next section). This peak has a width at half maximum of about 15% (in $\gamma\gamma$ collision) and photons here can have a high degree of polarization. In the next section it will be shown that in the current TESLA designs the $\gamma\gamma$ luminosity in the high energy peak can be up to 30-40% of the e^+e^- luminosity at the same beam energy.

2.1 Higgs boson

The present Standard Model (SM) assumes existence of a very unique particle, the Higgs boson, which is thought to be responsible for the origin of particle masses. It has not been found yet, but from existing experimental information it follows that, if it exists, its mass is higher than 112 GeV (LEP200) and is below 200 GeV [14], i.e. lays in the region of the next linear colliders. In the simplest extensions to the SM the Higgs sector consists of five physics states: h^0, H^0, A^0 and H^\pm . All these particles can be studied at photon colliders and some characteristics can be measured better than in e^+e^- collisions.

The process $\gamma\gamma \rightarrow H$ goes via the loop with heavy virtual charged particles and its cross section is very sensitive to the contribution of particles with masses far beyond the energies covered by present and planned accelerators [15]. If the Higgs is light enough, its width is much less than the energy spread in $\gamma\gamma$ collisions. The “effective” cross section with account of the energy spread is presented in Fig.2 [16]. Here $L_{\gamma\gamma}$ is defined as the $\gamma\gamma$ luminosity at the high energy peak of the luminosity spectrum. For comparison, the cross sections of the Higgs production in e^+e^- collisions are shown. We see that for $M_H = 120\text{--}250$ GeV the effective cross section in $\gamma\gamma$ collisions is larger than the sum of the cross sections in e^+e^- collisions by a factor of about 9–30. It can be detected as a peak in the invariant mass distribution or can be searched for by energy scanning using the very sharp ($\sim 1\text{--}2\%$) high energy edge of

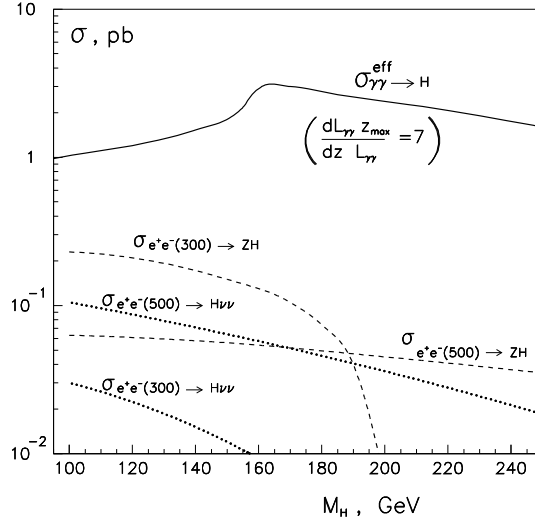


Fig. 2. Cross sections for the Standard model Higgs in $\gamma\gamma$ and e^+e^- collisions.

the luminosity distribution [16]. For the integrated luminosity 50 fb^{-1} (in the peak) the number of produced Higgs will be 50–150 thousands (depending on the mass).

At $M < 150 \text{ GeV}$ the Higgs decays mainly to b-quarks. The cross section of the process $\gamma\gamma \rightarrow H \rightarrow b\bar{b}$ is proportional to $\Gamma_{\gamma\gamma}(H) \times Br(H \rightarrow b\bar{b})$. The branching ratio $Br(H \rightarrow b\bar{b})$ can be measured with a high precision in e^+e^- collisions in the process with the "tagged" Higgs production: $e^+e^- \rightarrow ZH$ [17]. As a result, one can measure the $\Gamma_{\gamma\gamma}(H)$ width at photon colliders with an accuracy better than 2–3% [18–20]. This is sufficient for distinguishing between Higgs models [21].

Moreover in the models with several neutral Higgs bosons, heavy H^0 and A^0 bosons have almost equal masses and at certain parameters in the theory are produced in e^+e^- collisions only in associated production $e^+e^- \rightarrow HA$ [22], while in $\gamma\gamma$ collision they can be produced singly with sufficiently high cross section [23]. Correspondingly, in $\gamma\gamma$ collisions one can produce Higgs bosons with about 1.5 times higher masses.

2.2 Charge pair production

The second example is the charged pair production. It could be W^+W^- or $t\bar{t}$ pairs or some new, for instance, charged Higgs bosons or supersymmetric particles. Cross sections for the production of charged scalar, lepton, WW pairs in $\gamma\gamma$ collisions are larger than those in e^+e^- collisions by a factor of approximately 5–20. The corresponding graphs can be found elsewhere [9,3].

For scalar particle, the cross section in e^+e^- and $\gamma\gamma$ collisions is presented in

fig.3 [24]. One can see that the cross section in collisions of polarized photons for large masses (near the threshold) is higher than that in e^+e^- collisions by a factor of 20. In addition, near the threshold the cross section in the $\gamma\gamma$ collisions is very sharp, $\propto \beta$, while in e^+e^- it contains a factor β^3 ; this is useful for measurements of particle masses.

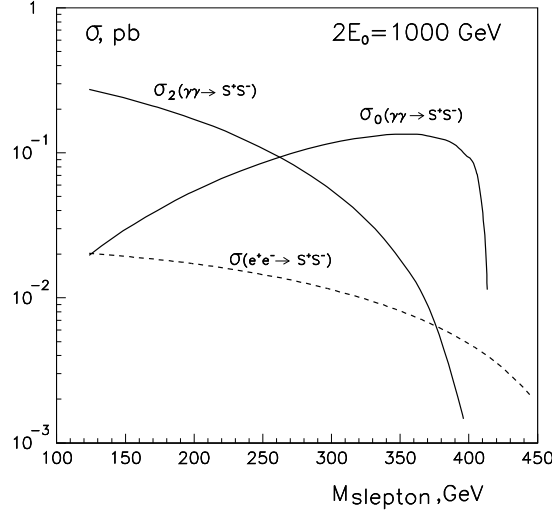


Fig. 3. Cross sections for charged scalars production in e^+e^- and $\gamma\gamma$ collisions at $2E_0 = 1$ TeV collider (in $\gamma\gamma$ collision $W_{max} \approx 0.82$ TeV, $x = 4.6$); σ_0 and σ_2 correspond to the total $\gamma\gamma$ helicity 0 and 2.

Note, that in e^+e^- collisions two charged pairs are produced both via annihilation diagram with virtual γ , Z and also via exchange diagrams where some new particles can give contributions, while in $\gamma\gamma$ collisions it is pure a QED process which allows the charge of produced particles to be measured unambiguously. This is a good example of complementarity in the study of the same particles in different types of collisions.

2.3 Accessible masses

In γe collisions, charged particle with a mass higher than that in e^+e^- collisions can be produced (a heavy charged particle plus a light neutral); for example, supersymmetric charged particle plus neutralino or new W boson and neutrino. Also, $\gamma\gamma$ collisions provide higher accessible masses for particles which are produced as a single resonance in $\gamma\gamma$ collisions (such as neutral Higgs bosons).

2.4 Search for anomalous interactions

Precise measurement of cross sections allow the observation of effects of anomalous interactions. The process $\gamma\gamma \rightarrow WW$ has large cross section (about 80 pb) and it is one of most sensitive processes for a search for a new physics (if no new particles are observed directly). The vertex γWW can be studied much better than in e^+e^- collisions because in the latter case the cross section is much smaller and this vertex gives only 10% contribution to the total cross section. The two factors together give about 40 times difference in the cross sections [25]. Besides that, in $\gamma\gamma$ collisions the $\gamma\gamma WW$ vertex can be studied.

2.5 Quantum gravity effects with Extra Dimensions

This new theory [26] suggests a possible explanation of why gravitation forces are so weak in comparison with electroweak forces. It is suggested that the gravitation constant is equal to the electroweak but in a space with extra dimensions. This extravagant theory can be tested at photon colliders and a two times higher mass scale than in e^+e^- collisions can be reached [27].

Many other examples can be found in these proceedings.

3 Possible luminosities of $\gamma\gamma, \gamma e$ collisions at TESLA

As it is well known in e^+e^- collisions the luminosity is restricted by beamstrahlung and beam instabilities. Due to the first effect the beams should be very flat. In $\gamma\gamma$ collisions these effects are absent, therefore one can use beams with much smaller cross section. Limitations of the luminosity at photon colliders are discussed in section 3.2. At present TESLA beam parameters the $\gamma\gamma$ luminosity is determined only by the attainable geometric L_{ee} luminosity. Below we consider first currently possible luminosity and then fundamental limitations.

3.1 Luminosities in the current design

What luminosity can be obtained with available technologies? It depends on emittances of electron beams. There are two methods of production low-emittance electron beams: damping rings and low-emittance RF-photo-guns (without damping rings). The second option is promising, but at this moment

there are no such photo-guns producing polarized electron beams [28]. Polarization of electron beams is very desirable for photon colliders [7], because: a) it increases the luminosity in the high energy peak by a factor of 3–4; b) polarization characteristics of high energy photons are better (broader part of spectrum have high degree of polarization). So, there is only one choice now — damping rings.

Specially for photon collider the TESLA group has studied the possibility of decreasing emittances at the TESLA damping ring. Preliminary, very encouraging results were reported at the workshop. After some additional check the new parameters of TESLA damping ring are presented in W.Decking's paper in these proceedings [29]. The conclusion is that the horizontal emittance can be reduced by a factor of 4 in comparison with the previous design.

The luminosity depends also on β -functions at the interaction points: $L \propto 1/\sqrt{\beta_x \beta_y}$. Vertical β_y is usually close to the bunch length σ_z . It is so for e^+e^- collisions and can be done for $\gamma\gamma$ collisions as well. Some questions remain on the minimum horizontal β -function. For e^+e^- collisions $\beta_x \sim 15$ mm, much larger than the beam length $\sigma_z = 0.3$ mm because beams in e^+e^- collisions must be flat to reduce beamstrahlung. In $\gamma\gamma$ collisions, β_x could be about 1 mm (or even somewhat smaller). There are two fundamental limitations: the beam length and the Oide effects [30] (radiation in final quads), the latter is not important for considered beam parameters. There is also some problem with the angular spread of the synchrotron radiation emitted in final quads. But, for the photon collider we are going to use the crab-crossing scheme and in this case there is sufficient clear angle for removal of the disrupted beams and synchrotron radiation.

However, very preliminary study of the existing scheme of the TESLA final focus has shown [31] that it does not work properly at β_x less than about 6 mm due to chromo-geometric abberations. This value is not fundamental and it is very likely that after further study and optimization a better solution will be found. Besides that, at SLAC recently a new scheme for the final focus system has been proposed [32]. The first check without optimization has shown [33] that with the new scheme one can obtain $\beta_x = 2$ mm without abberations. With this level of uncertainty I will assume $\beta_x = 1.5$ mm for this paper .

Some uncertainties remain also for operation of the TESLA at low energies. In the case of $M_H = 130$ GeV the required electron beam energy lies between 79 GeV (for $x = 4.6$, $\lambda = 0.325 \mu\text{m}$) and 100 GeV (for $x = 1.8$, $\lambda = 1.06 \mu\text{m}$). In this case TESLA should work at lowered accelerating gradient or use bypass. If one use the same electron bunches and the same beam-train structure and the repetition rate, the luminosity will be proportional to the beam energy E_0 (because $L \propto 1/\sigma_x \sigma_y$ and $\sigma_i \propto \sqrt{\epsilon_i}$ and $\epsilon_i = \epsilon_{ni}/\gamma$).

In principle, this loss of luminosity can be compensated by increase of the repetition rate as $f \propto 1/E_0$, in this case the RF power (for linac) is constant. Unfortunately, for the present design of the TESLA damping ring the repetition rate may be increased only a factor of 2 due to a smaller damping time for electron beams. Further decrease of the damping time is possible but add additional cost (wiggler, RF-power).

Other problem of working at low gradients is the beam loading problem (RF efficiency). Its adjustment requires change of a coupler position, which is technically very difficult or even impossible.

Due to these uncertainties TESLA accelerator physicists have recommended to use the scaling $L \propto E$. However, if the low mass Higgs is found, some solutions for increasing luminosity at low energies can be found. For this paper I assume the same beam parameters for all energies, that gives $L \propto E$.

The resulting parameters of the photon collider at TESLA for $2E=500$ GeV and $H(130)$ are presented in Table 1. It is assumed that electron beams have 85% longitudinal polarization and laser photons have 100% circular polarization. The thickness of laser target is one collision length (so that $k^2 \approx 0.4$). The conversion point (CP) is situated at the distance $b = \gamma\sigma_y$ from the interaction point.

Table 1

Parameters of the $\gamma\gamma$ collider based on TESLA. Left column for $2E=500$ GeV, next two columns for Higgs with $M=130$ GeV, two options.

	2E=500	2E=200	2E=158
	$x = 4.6$	$x = 1.8$	$x = 4.6$
$N/10^{10}$	2	2	2
σ_z , mm	0.3	0.3	0.3
$f_{rep} \times n_b$, kHz	14.1	14.1	14.1
$\gamma\epsilon_{x/y}/10^{-6}$, m·rad	2.5/0.03	2.5/0.03	2.5/0.03
$\beta_{x/y}$, mm at IP	1.5/0.3	1.5/0.3	1.5/0.3
$\sigma_{x/y}$, nm	88/4.3	140/6.8	160/7.6
b, mm	2.1	1.3	1.2
L_{ee} (geom), 10^{33}	120	48	38
$L_{\gamma\gamma}(z > 0.8z_{m,\gamma\gamma})$, 10^{33}	11.5	3.5	3.6
$L_{\gamma e}(z > 0.8z_{m,\gamma e})$, 10^{33}	9.7	3.1	2.7
θ_{max} , mrad	9	8.5	16

For the Higgs the production rate is proportional to dL_0/dW at $W = M_H$. For the considered cases, $M_H = 130$ GeV, $x = 4.6$ and $x = 1.8$, $dL_0/dW = 1.65 \times 10^{32}$ /GeV and 1.5×10^{32} /GeV, respectively, so that the coefficient in Fig.2 characterizing the width of the peak is about 5.9 and 5.5 (instead of 7).

Using these luminosities and Fig. 2 one can find that the rate of production of the SM Higgs boson with $M_H=130(160)$ GeV in $\gamma\gamma$ collisions is 0.9(3) of that in e^+e^- collisions at $2E = 500$ GeV (both reactions, ZH and $H\nu\nu$).

Comparing the $\gamma\gamma$ luminosity with the e^+e^- luminosity ($L_{e^+e^-} = 3 \times 10^{34}$ $\text{cm}^{-2}\text{s}^{-1}$ for $2E = 500$ GeV [34]) we see that for the same energy

$$L_{\gamma\gamma}(z > 0.8z_m) \sim 0.4L_{e^+e^-}. \quad (2)$$

For example, as we have seen (Fig.3) the cross section for production of H^+H^- pairs in collisions of polarized photons is higher than that in e^+e^- collisions by a factor of 20 (not far from the threshold); this means 8 times higher production rate for the luminosities given above.

The relation (2) is valid only for the considered beam parameters. A more universal relation is (for $k^2 = 0.4$)

$$L_{\gamma\gamma}(z > 0.8z_m) \sim 0.1L_{ee}(\text{geom}). \quad (3)$$

The normalized $\gamma\gamma$ luminosity spectra for $2E_0 = 500$ GeV are shown in Fig.4.

The luminosity spectrum is decomposed into two parts, with the total helicity of two photons 0 and 2. We see that in the high energy part of the luminosity spectra photons have a high degree of polarization. In addition to the high energy peak, there is a factor 5–8 larger low energy luminosity. It is produced mainly by photons after multiple Compton scattering and beamstrahlung photons. These events have a large boost and can be easily distinguished from the central high energy events. In the same Fig.4 you can see the same spectrum with an additional cut on the longitudinal momentum of the produced system which suppresses low energy luminosity to a low level. For two jet events ($H \rightarrow b\bar{b}$, $\tau\tau$, for example) one can restrict the longitudinal momentum using the acollinearity angle between jets. The resulting monochromaticity of collisions will be about 7.5 %, see Fig.4 (lower).

The high energy part of the $\gamma\gamma$ luminosity spectrum is almost independent on collision effects at the IP (beamstrahlung and multiple Compton scattering). For theoretical studies one can obtain it with sufficient accuracy by convolution of the Compton function [7]. Recently, a simple analytical formula for the Compton function has been obtained [35] which takes into account non-linear effects in the conversion region for small enough values of ξ^2 . At photon colliders it is about 0.2–0.3 in the center of the laser focus. In the simulation one has also to take into account variation of ξ^2 in the conversion region. As a good approximation one can generate "t" distributed by the Gaussian law and then calculate $\xi^2 = \xi_0^2 \exp(-t^2/2)$.

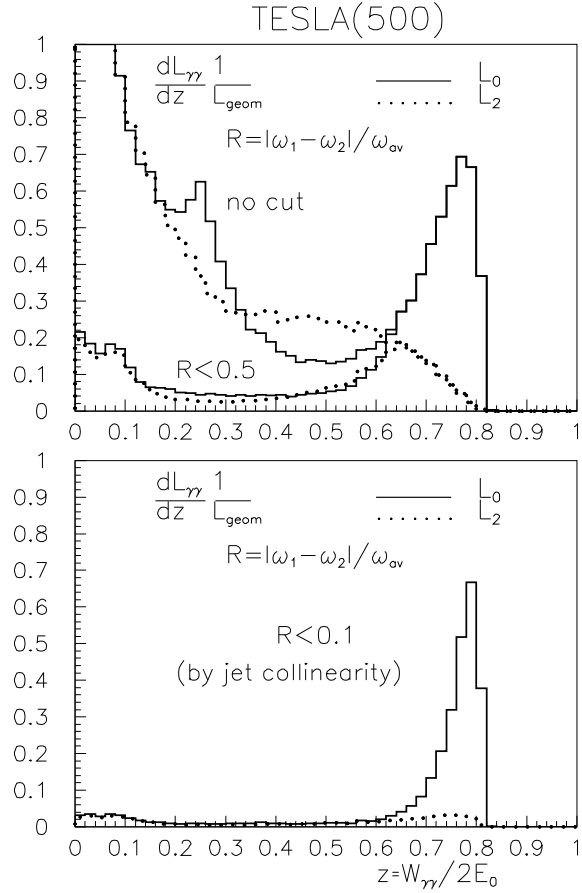


Fig. 4. $\gamma\gamma$ luminosity spectra at TESLA(500) with various cuts on longitudinal momentum. Solid line for total helicity of two photons 0 and dotted line for total helicity 2. See comments in the text.

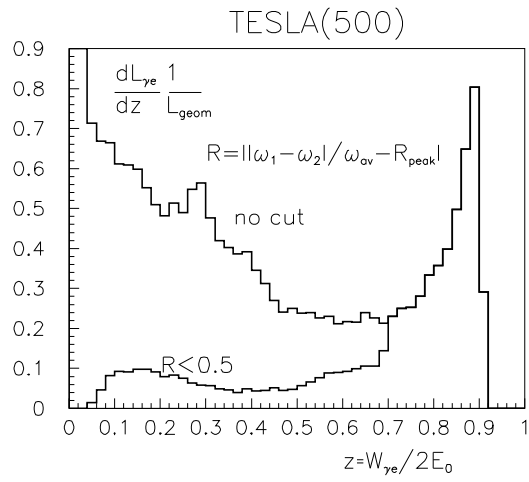


Fig. 5. Normalized γe luminosity spectra at TESLA(500) for parameters given in Table 1. See comments in the text.

The normalized γe luminosity spectra for $2E=500$ GeV are shown in Fig.5. Again, beside the high energy peak there is a several times larger γe luminosity at low invariant masses. Note, that γe luminosity in the high energy peak is not a simple geometric characteristic of the Compton scattering (as it is in $\gamma\gamma$ collisions). For the considered case it is suppressed by a factor of 2–3, mainly due to repulsion of the electron beams and beamstrahlung. The suppression factor depends strongly on beam parameters. Note, that for a special experiment on QCD study at low luminosity one can increase the distance between the conversion and interaction points and obtain very monochromatic γe luminosity spectrum with a small low energy background. This is due to the effective transverse magnetic field in the detector solenoid which acts on the beam in the case the crab crossing collisions.

The luminosity distributions for the case of Higgs (130 GeV) are presented in fig.6. All parameters for this figure are given in Table 1. Two cases are considered: $E=79$ GeV, $x \sim 4.6$ ($\lambda = 0.325 \mu\text{m}$) and $E=100$ GeV, $x = 1.8$ ($\lambda = 1.06 \mu\text{m}$, which corresponds to wave lengths of the most power solid state lasers).

Beside the convenience of using the same laser with $\lambda \sim 1 \mu\text{m}$ for all energies there are two other advantages of the latter case. For measurement of the Higgs bosons CP parity a linear polarization of high energy photons is required [36,37]. Maximum value of the linear polarization is $l_\gamma = 2/(1 + x + (1 + x)^{-1})$ [7], it is 63.3 % for $x = 1.8$ and only 33.5 % for $x = 4.8$. Second advantage of $x = 1.8$ are smaller disruption angles of the beams after collisions, see table 1. The disruption angle and the angular size of the first quadrupole determine the value of the crab crossing angle (fig.1). In the present design $\alpha_c = 34$ mrad (angle between electron beams). It may be not sufficient for collisions of 80 GeV electron beams and $x = 4.6$. One can use here $\lambda \sim 1 \mu\text{m}$ or $\lambda \sim 0.5 \mu\text{m}$ (doubled frequency).

Several other important accelerator aspects of the photon collider at TESLA are discussed in N.Walker's talk at this workshop [31].

3.2 *Ultimate $\gamma\gamma$ luminosity*

There is only one collision effect restricting the $\gamma\gamma$ luminosity, that is a process of coherent pair creation when the high energy photon is converted into an e^+e^- pair in the strong field of the opposing electron beam [38],[8],[9]. In γe collisions, beside coherent pair creation, two other effects are important: beamstrahlung (electrons of the “main” electron beam radiate in the field of the electron beam used for photon production) and repulsion of beams.

Below are results of simulations with the code which takes into account all

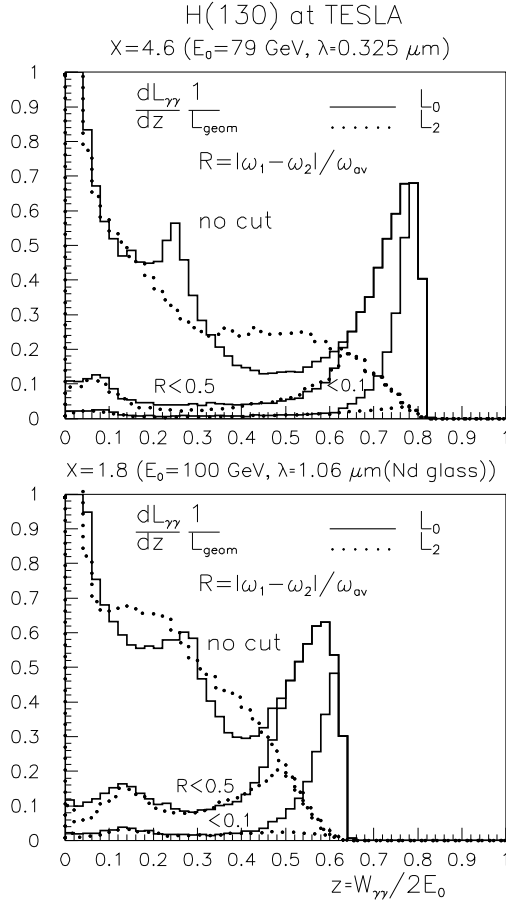


Fig. 6. $\gamma\gamma$ luminosity spectra at the photon collider for study of the Higgs with the mass $M_H = 130$ GeV; upper figure for $x = 4.6$ and lower one for $x = 1.8$ (the same laser as for $2E_0 = 500$ GeV). See also Table 1.

main processes in beam-beam interactions [9]. Fig.7 shows dependence of the $\gamma\gamma$ (solid curves) and γe (dashed curves) luminosities on the horizontal beam size for TESLA beam parameters at several energies. The horizontal beam size was varied by change of horizontal beam emittance keeping the horizontal beta function at the IP constant and equal to 1.5 mm.

One can see that all curves for $\gamma\gamma$ luminosity follow their natural behavior: $L \propto 1/\sigma_x$ ($\sigma_x < 10$ nm are not considered because too small horizontal sizes may have problems with crab-crossing). Note that in e^+e^- collisions $\sigma_x \sim 500$ nm. In γe collisions the luminosity is lower than in $\gamma\gamma$ collisions due to the displacement of the electron beam during the beam collision and beamstrahlung. So, we can conclude that for $\gamma\gamma$ collisions one can use beams with the horizontal beam sizes much smaller than those in e^+e^- collisions. Note, that photon colliders can have two times smaller vertical beam size than it is now in TESLA (for even smaller electron beam size the effective photon beam size will be determined by the Compton scattering contribution). As result, the $\gamma\gamma$ luminosity in the high energy peak can be, in principle, several times higher

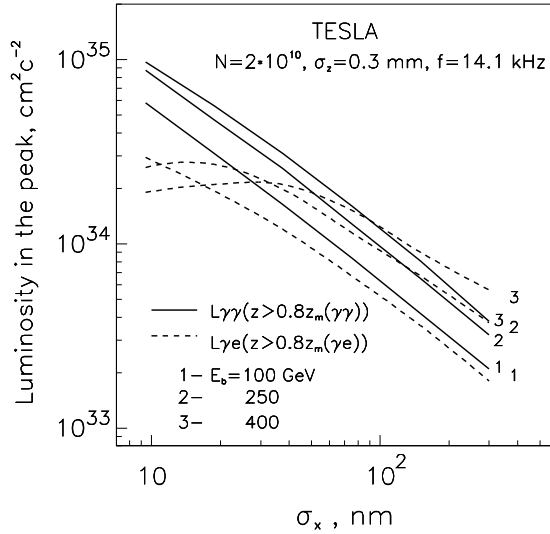


Fig. 7. Dependence of $\gamma\gamma$ and γe luminosities in the high energy peak on the horizontal beam size for TESLA at various energies. See also comments in the text.

than that in e^+e^- collisions ($L_{e^+e^-} = 3 \times 10^{34}$ at $2E=500$ GeV [34]).

This would be great because the cross sections in $\gamma\gamma$ collisions also are by one order larger. However, there is one problem: we don't know now how to prepare electron beams with so small horizontal emittances. There is one method, laser cooling [39–41] which allows, in principle, to reach the required emittances, but it is very challenging technically and needs many years of studies, before we can consider it seriously.

4 Lasers, optics

A key element of photon colliders is a powerful laser system which is used for $e \rightarrow \gamma$ conversion. Lasers with the required flash energies (several J) and pulse duration ~ 1 ps already exist and are used in several laboratories. The main problem is the high repetition rate, about 10–15 kHz, with a pulse structure repeating the time structure of the electron bunches.

A very promising way to overcome this problem at TESLA is an “external optical cavity” approach which allows a considerable reduction of the required peak and average laser power [24]. Technical aspects of this approach are considered by I.Will and his colleagues at this Workshop [42].

Another possible solution is a one-pass free electron laser. Recently, first such laser has been successfully commissioned at DESY [43]. This option is described by M.Yurkov and colleagues [44] at this Workshop.

However, the most attractive and reliable solution at this moment is an “optical storage ring” with a diode pump laser injector which, it seems, can be build already now. This new approach can be considered as a base-line solution for the TESLA photon collider.

4.1 Requirements for the laser, wave length, flash energy

The processes in the conversion region, i.e. Compton scattering and several other important phenomena, have been considered in detail in papers [6–9,40,45] and references therein. Laser parameters important for this task are: laser flash energy, duration of laser pulse, wave length and repetition rate. The requirement for the wave length was considered in the introduction. The optimum value for TESLA(500) is $\lambda \sim 1 \mu\text{m}$.

In the calculation of the required flash energy one has to take into account the natural “diffraction” emittance of the laser beam [6] and nonlinear effects in the Compton scattering. The nonlinear effects are characterized by the parameter $\xi^2 = e^2 \bar{B}^2 \hbar^2 / (m^2 c^2 \omega_0^2)$ [46] (ω_0 is the energy of laser photons). Due to nonlinear effects the high energy peak in the Compton spectrum is shifted to lower energies: $\omega_m/E_0 = x/(x + 1 + \xi^2)$, this leads also to broadening of the high energy edge of the luminosity spectrum. Therefore $\xi^2 < 0.2 - 0.3$ is required [9].

The result of MC simulation of k^2 (k is the conversion coefficient) for the electron bunch length $\sigma_z = 0.3 \text{ mm}$ (TESLA project), $\lambda = 1.06 \mu\text{m}$, $x = 4.8$ as a function of the Rayleigh length (β -function of the laser beam at a focal point) for various flash energies and values of the parameter ξ^2 (in the center of the laser bunch) are shown in fig.8.

It was assumed that the angle between the laser optical axis and the electron beam line is $\theta = 2\sigma_{L,x'}$ ($\sigma_{L,x'}$ is the angular divergence of the laser beam in the conversion region), so that the mirror system is situated outside the electron beam trajectories. One conversion length corresponds to $k^2 = (1 - e^{-1})^2 \approx 0.4$. One can see that $k^2 = 0.4$ at $\xi^2 = 0.3$ can be achieved with the minimum flash energy $A = 5 \text{ J}$. The optimum value of the Rayleigh length is about 0.35 mm.

The r.m.s. duration of the laser pulse can be expressed via other laser parameters defined above [13]

$$\sigma_{L,z} = \frac{4r_e \lambda A}{(2\pi)^{3/2} mc^2 \xi^2 Z_R} = 9.3 \times 10^{-5} \frac{A[\text{J}]}{Z_R[\text{cm}] \xi^2} \text{ cm}, \quad (4)$$

where the last equality corresponds to $\lambda = 1.06 \mu\text{m}$. For $\xi^2 = 0.3$ and $Z_r = 0.35$

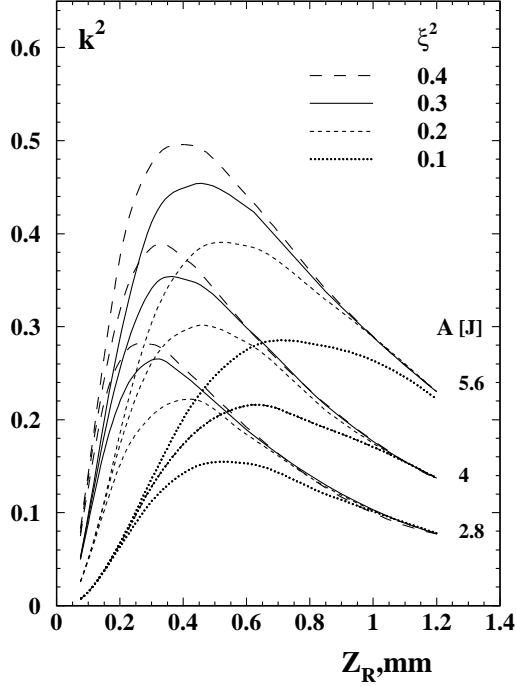


Fig. 8. Square of the conversion probability (proportional to the $\gamma\gamma$ luminosity) as a function of the Rayleigh length for various parameters ξ^2 and laser flash energies, $x = 4.8$, $\lambda = 1.06 \mu\text{m}$ are assumed. The mirror system is situated outside the electron beam trajectories (collision angle $\theta = 2\sigma_{L,x'}$). The crab crossing angle 30 mrad is taken into account. See also the text.

mm the optimum length of the laser bunch is $\sigma_{L,z} = 0.44$ mm or 1.5 ps.

The angular size of the focusing mirror is taken to be equal to two r.m.s. angular spread (in x or y directions) at the conversion point [6]

$$\Delta\theta_m = \pm 2\sigma_{L,x'} = \pm 2\sqrt{\frac{\lambda}{4\pi Z_R}} = \pm 0.031. \quad (5)$$

The ratio of the focal distance to the mirror diameter ($f_\#$) is equal to $1/(2 \times 0.031) \approx 16$. For $L = 2$ m, $d = 12.5$ cm. The fluence (A/cm^2) in the center of the mirror is $A/(2\pi\sigma_x^2) = 8A/(\pi d^2) \sim 0.082 \text{ J/cm}^2$, while the damage threshold is in the range 0.7–2 J/cm²[1]. In addition to the final focusing mirror the optics inside the detector contains another mirror with about two times smaller diameter [13] (see also fig.9). The corresponding fluence on this mirror is four times higher, about 0.3 J/cm². In the case of flattop laser beams approximately similar beam sizes in focus are obtained when the $f_\#$ of the flattop beam is about 0.7 times that of the Gaussian beam [1]. The fluence on the mirrors will be about 4 times smaller (due to larger area and uniform distribution).

In summary: the required laser wavelength is about 1 μm , flash energy is

5 J, the repetition rate of about 14 kHz, so the average power of the laser system should be about 70 kW each of two lasers. Besides, at TESLA the laser should work only 0.5 % of the time: one train of 1 msec duration contains 3000 bunches, the repetition rate is 5 Hz. Non-uniformity of LC operation (the train structure) is a very serious complication.

Below we will consider three variants of laser system: optical storage ring, external optical cavity, free-electron laser. Present technique of short pulse powerful solid state lasers is based on the following modern technologies: pulsed-chirped techniques, diode pumping, adaptive optics. Discussion of laser technologies for photon colliders can be found elsewhere [1].

4.2 *Optical storage ring*

To overcome the “repetition rate” problem it is quite natural to consider a laser system where one laser bunch is used for $e \rightarrow \gamma$ conversion many times. Indeed, 5 J laser flash contains about 5×10^{19} laser photons and only $10^{10} - 10^{11}$ photons are knocked out in one collision with the electron bunch. Below two ways of multiple use of one laser pulse is considered. The first one is shown in fig. 9.

In fig.9a the laser pulse is used twice for $e \rightarrow \gamma$ conversion. After the collision with the electron beam (number 1) the laser beam exits from the detector and after a 337 ns loop (the interval between beam collisions at TESLA) returns back and collides with the opposite electron beam (number 2). The second pass does not need any special optical elements, only mirrors. This is a very natural and simple solution. In this scheme the laser system should generate bunches with an interval of 337 ns.

In fig.9b the laser pulse is used for conversion four times. In this scheme one additional optical element is used, a thin film polarizer (TFP), which is transparent for the light polarized in the plane of the paper and reflects the light with the orthogonal polarization. Directions of the polarization during the first cycle are shown in fig.9b. After the first cycle the polarization is perpendicular to the paper and the light is reflected from the TFP, while after the second cycle the polarization will be again in the plane of the paper and the laser pulse will escape the system via the TFP. The laser bunches are emitted by the laser at an interval of 2×337 ns.

In fig.9c the laser pulse is sent to the interaction region where it is trapped in an optical storage ring. This can be done using Pockels cells (P), thin film polarizers (TFP) and 1/4-wavelength plates ($\lambda/4$). Each bunch makes several (n) round trips and then is removed from the ring. All these tricks can be done by switching one Pockels cell which can change the direction of linear

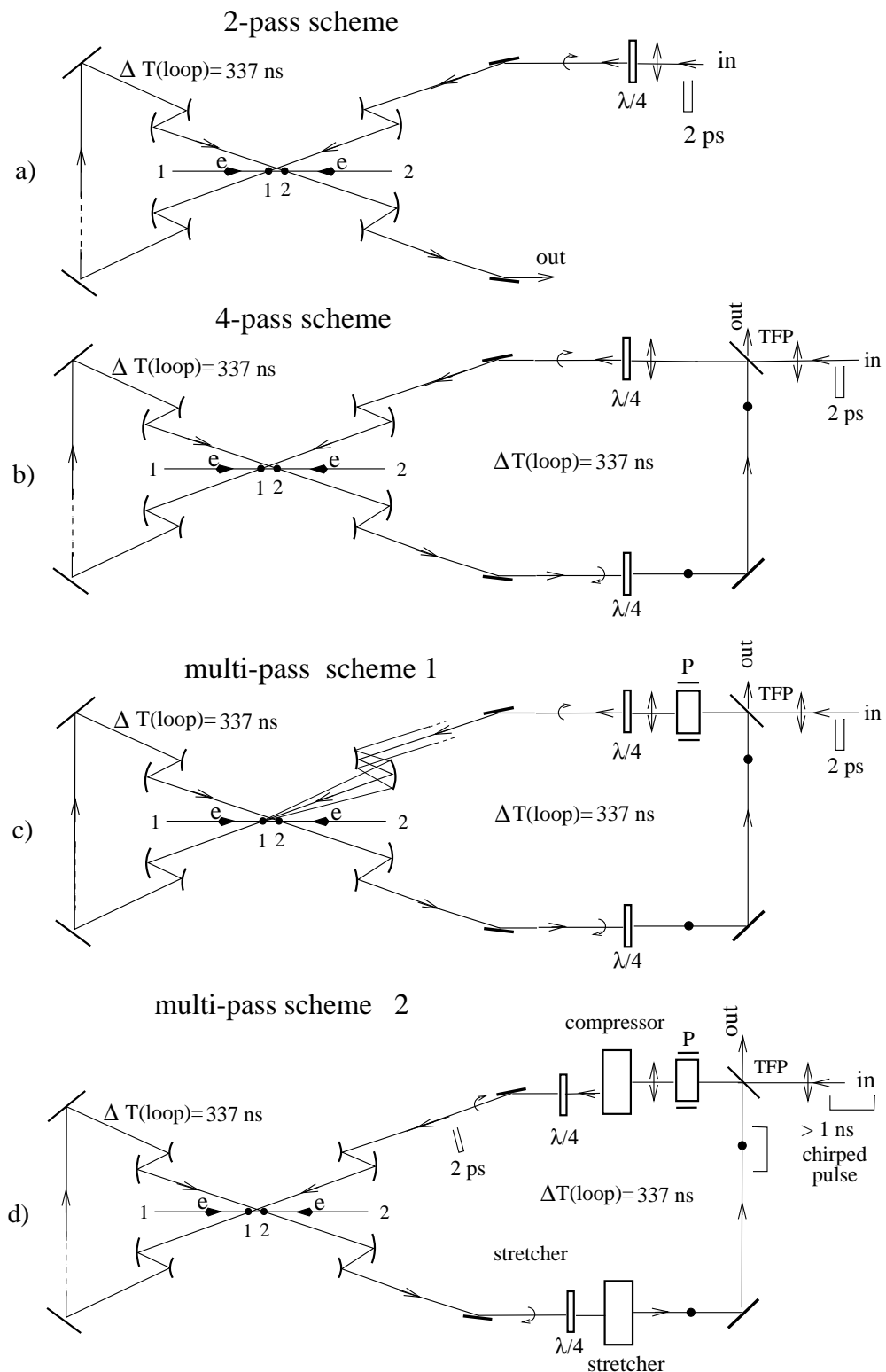


Fig. 9. Optical trap: a) 2-pass optics for $e \rightarrow \gamma$ conversions; b) 4-pass optics; c) optical storage ring without stretching-compression; d) optical storage ring with stretching-compression; P is a Pockels cell, TFP is a thin film polarizer, thick dots and double arrows show the direction of polarization.

polarization by 90 degrees. The $\lambda/4$ plates are used for obtaining circular polarization at the collision point. For obtaining linear polarization at the IP these plates should be replaced by $1/2$ wavelength plates. A similar kind of optical trap was considered as one of the options in the NLC Zero-design report [1]. The number of cycles is determined by the attenuation of the pulse and by nonlinear effects in optical elements. The latter problem is very very serious for TW laser pulses. During one total loop each bunch is used for conversion twice (see Fig.9c). The laser bunch is collided first with electron beam 1 traveling to the right and after a time equal to the interval between collisions (333 ns) it is collided with beam 2 traveling to the left. This does not work (i.e. there are no $\gamma\gamma$ collisions) for the first $n/2 \sim 5$ collisions, when there is only one laser bunch in the loop, but this is not a problem because there are 3000 collision during the train (the same is valid also for two previous schemes).

In fig.9d the laser pulse is trapped in the same way as in fig.9c, but to avoid the problems of non-linear effect (self-focusing) in the optical elements, a laser pulse is compressed before the collision with the electron bunch down to about 2–3 ps using grating pairs, it is then stretched again up to the previous length of about 1 ns just before passing through the optical elements.

Which system is better, 9c or 9d, is not clear apriori. In the scheme (c) the number of cycles is limited by nonlinear effects, in the scheme (d) additional attenuation is added by the gratings used for compression and stretching. Optical companies suggest gratings for powerful lasers with $R \sim 95\%$. One round trip needs four gratings, this means 20% loss/trip. So, the maximum number of trips is only about two. This makes no sense because the scheme 9b is simpler and also allows two cycles. My guess is that a reflectivity of 95% for gratings is not the limit and one should not exclude the scheme with the compression-stretching from consideration.

How large can the decrease of the laser energy per round trip be in the scheme without bunch compressor-stretchers? The minimum number of mirrors in the scheme is about 15–20. Reflectivity of multilayer dielectric mirrors for large powers suggested by optical companies is about 99.8%. So, the total loss/cycle is about 3–4%. Let us add 1% attenuation in the Pockels cell. Due to the decrease of the laser flash energy the luminosity will vary from collision to collision. Calculation shows that for 1.3, 1.4, 1.5 times attenuation of the laser pulse energy before the pulse is replaced, the $\gamma\gamma$ luminosity will vary on 14, 17, 21 % only (here we assumed that on average the thickness of the laser target is one collision length). For 5% loss/turn and 6 round trips the attenuation is 1.35, which is acceptable.

Let us consider the problem of nonlinear effects for the scheme 9c. The refrac-

tive index of the material depends on the beam intensity

$$n = n_0 + n_2 I. \quad (6)$$

This leads to self focusing of the laser beam [47]. There are two kinds of self-focusing. The first type is a self-focusing of the beam as a whole. The second one is self-focusing and amplification of irregularities which leads to break up of the beam into a large number of filaments with the intensity exceeding the damage level. Both these effects are characterized by the parameter B-integral [47,1]

$$B = \frac{2\pi}{\lambda} \int \Delta n dl = \frac{2\pi}{\lambda} n_2 I_{peak} L \quad (7)$$

If the beam has a uniform cross section then nonlinear effects do not lead to a change of the beam profile, while for the Gaussian like beam $B \sim 1$ means that the self-focusing angle is approximately equal to the diffraction divergence of the beam. This is not a problem, such kind of distortions can be easily corrected by adaptive optics.

The second effect is more severe. Even for uniform (in average) distribution of the intensity over the aperture a small initial perturbation δI grows exponentially with a rate depending on the spatial wave number.² The maximum rate is given by the same parameter B [47]

$$\delta I = \delta I_0 e^B. \quad (8)$$

This is confirmed experimentally. To avoid small-scale growth the parameter B should be smaller than 3–4 [47,1], in other words

$$I_{peak} < \frac{\lambda}{2n_2 L} \quad (9)$$

Now we can get the relationship between the diameter and the maximum thickness of the material. For $A = 5 \text{ J}$, $\lambda = 1 \mu\text{m}$, $\sigma_{L,z} = 1.5 \text{ ps}$ and a typical value of $n_2 \sim 3 \times 10^{-16} \text{ cm}^2/\text{W}$ (I have not found n_2 for KD*P used for Pockels cells) and flat-top beam we get

$$L[\text{cm}] < 0.1 S[\text{cm}^2]. \quad (10)$$

² Such instability exists when total beam power exceeds the threshold power for the medium, which is of the order of one MW [47], that is 6 orders lower than the power needed for photon colliders

For a beam diameter of 15 cm we obtain $L < 17$ cm. For Gaussian beams the maximum thickness is about two times smaller.

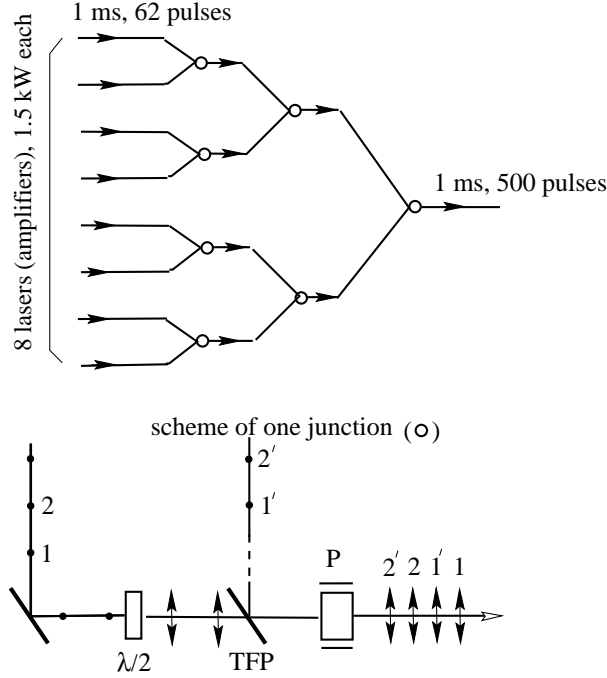
What is L ? Is it the maximum thickness of one optical element, the thickness integrated over the loop or the previous one times the number of round trips? In the scheme 9c the dominant contribution to the total thickness is given by the Pockels cell. After the Pockels cell one can put a spatial filter and thus suppress the growth of spikes. So, L in our case is the thickness of the Pockels cell and it does not depend on the number of round trips. Moreover, our laser pulse is very short, has a broad spectrum and the corresponding coherence length is small, about $l_c \sim 4\pi\sigma_{L,z} \sim 0.5$ cm. The instabilities upon a uniform high intensity background developeds due to interference of fluctuation with the main power. However, this coherence is lost after the coherence length. In my opinion, the B-integral does not characterise the exponential growth of irregularities once the coherence length is much lower than L . So, it seems, that the problem of nonlinear effects in the scheme 9c is not dramatic. Construction of a Pockels cell with an aperture of about 10–15 cm and switching time 300 ns is not a very difficult problem. Quarter- and half-wave plates can be made thin or even joined with mirrors (retarding mirror).

In conclusion, it seems, that the optical scheme 9c with about 6 round trips (12 collisions with electron beams) is a very attractive and realistic solution for the TESLA photon collider.

Now a few words on a laser system required for a such an optical storage ring with 6 round trips. Schematically it is shown in fig.10. At the start (this is not shown) low-power laser produces a train of 1 msec duration consisting of 500 chirped pulses with duration several ns each. Then these pulses are distributed between 8 final amplifiers (see fig.) Each of the 8 sub-trains have a duration of 1 ms and consist of 62 pulses. After amplification up to the energy 5 J in one pulse these sub-trains are recombined to reproduce the initial time structure. The time spacing between bunches in the resulting train is equal to the 6 intervals between beam collisions in TESLA.

Due to the high average power the lasers should be based on diode pumping. Diodes have much higher efficiency than flash lamps, about $\epsilon \sim 25\%$ for single pulses. For pulse train (as it is in our case) it should be at least by factor of two higher. Besides that, diodes are much more reliable. This technology is developed very actively for other application, such as inertial fusion.

Main problem with diodes is their cost. Present cost of diode lasers is about 5\$ per Watt [48]. Let us estimate the required laser power. In the case of TESLA, the duration of the pulse train $T_0 = 1$ msec is approximately equal to the storage time ($\tau \sim 1$ msec) of the most promising powerfull lasers crystal, such as Yb:S-FAP, therefore, the storage time does not help at TESLA. The



required power of the diode pumping is

$$P_{diode} = \frac{A(\text{flash})N(\text{bunches})}{\epsilon T_0} = \frac{5 \text{ J} \times 500}{0.5 \times 10^{-3}} = 5 \text{ MW.} \quad (11)$$

Correspondingly, the cost of such diode system will be 25 M\$. Here we assumed 6-fold use of one laser bunch as described above. We see that even without Pockels cell (the scheme 9b with two round trips) the diode power is 15 MW and the cost of diodes is then 75 M\$, 1–2 percents of the LC cost.

Livermore laboratory is working now on the project of the inertial confinement fusion with a high repetition rate and efficiency with a goal to build a power plant based on fusion. This project is based on diode pumped lasers. According to ref.[49] they are currently working on the “integrated research experiment” for which “the cost of diodes should be reduced down to 0.5\$/Watt and the cost of diodes for fusion should be 0.07\$/Watt or less.” So, perspectives of diode pumped lasers for photon colliders are very promising. With 1\$/Watt the cost of diode is 5 M\$ for 6 round trips (with Pockels cell) and 15 M\$ for 2 round trips without Pockels cell. These numbers are reasonable even after multiplying by a safety factor 2–3.

Average output power of all lasers in the scheme 9c is about 12 kW, 1.5 kW for each laser.

4.3 “External” optical cavity

One of the problems in the optical traps at photon colliders is self-focusing in optical elements due to very high pulse power. In the case of the optical storage ring considered above, we avoid this problem by using compression-stretching of the laser pulses. Besides that, there is one way to “create” a powerful laser pulse in the optical “trap” without any material inside: laser pulse stacking in an “external” optical cavity [24].

Briefly, the method is the following. Using the train of low energy laser pulses one can create in the external passive cavity (with one mirror having some small transparency) an optical pulse of the same duration but with the energy by a factor of Q (cavity quality factor) higher. This pulse circulates many times in the cavity each time colliding with electron bunches passing the center of the cavity. For more details see ref. [24].

A possible layout of the optics at the interaction region scheme is shown in Fig.11. In this variant, there are two optical cavities (one for each colliding electron beam) placed outside the electron beams. Such a system has mini-

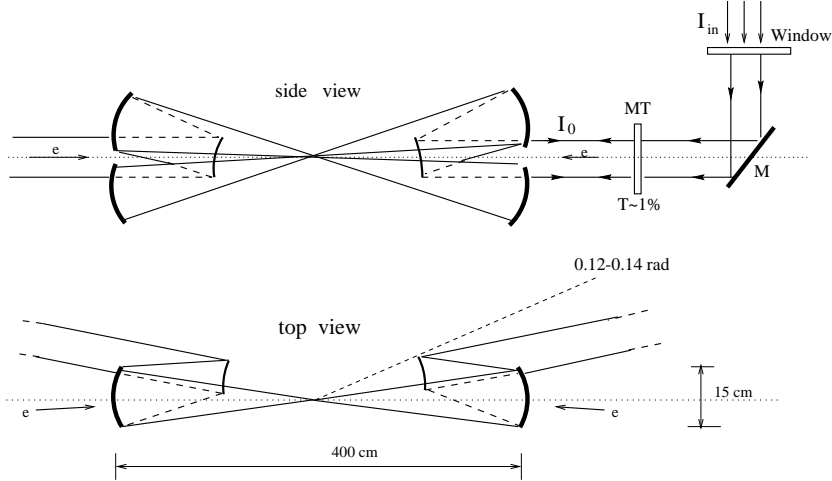


Fig. 11. One of possible scheme of optics at the IR.

mum numbers of mirrors inside the detector. One of several possible problems in such linear cavity (pointed out by I.Will at this workshop [42]) is back-reflection, in a ring type cavity this problem would be much easier. A possible scheme of such a ring cavity for photon colliders is shown in fig.12 (only some elements are shown).

More detailed technical aspects of the external cavity approach were discussed by I.Will and colleagues at this workshop [42]. Such a cavity is operated already in their institute and a $Q \sim 100$ has been demonstrated. In their opinion,

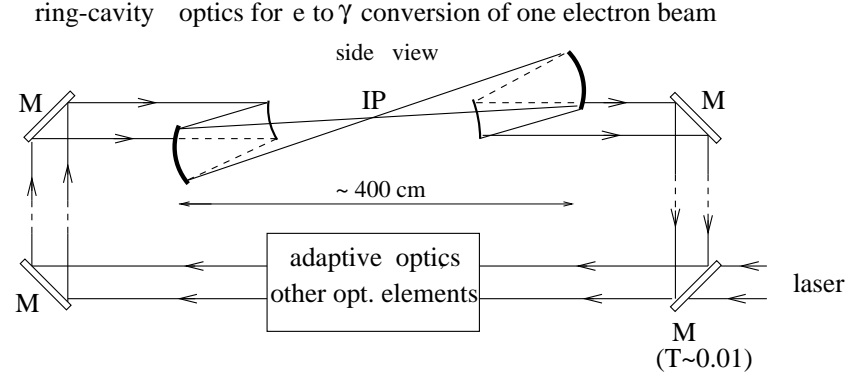


Fig. 12. Ring type cavity. Only the cavity for one electron beam is shown. Top view is quite similar to that in fig.11

the laser system with the optical cavity required for the photon collider can be made, though this task is much more difficult due to the much higher powers.

Comparing the optical cavity approach with the “optical trap” (or “optical storage ring”) considered in previous subsection, I would say that the optical cavity is very attractive but less studied. Here all tolerances should be of the order $\lambda/(2\pi Q)$, while in the optical trap they are much more relaxed, about $0.2\sigma_z/Q$, difference 300 times for the same Q !

4.4 Free electron lasers

Another approach for a laser for the TESLA photon collider is a free electron laser [44]. Recently DESY has demonstrated operation of a one pass FEL with the wave length $0.1 \mu\text{m}$ and further goal is 1 nm (this is included in TESLA proposal). Generation of $1 \mu\text{m}$ light is much a simpler task. However this task is also not simple because to obtain the required flash energy a very large part of the electron beam energy should be converted to light.

Summary: we have considered 3 possible options of laser system for TESLA photon collider:

- (1) Optical trap (storage ring) with about 8 diode pumped driving lasers (final amplifiers) with total average power about 7 kW. Beams are merged using Pockels cells and thin-film polarizers. This can be done now: all technologies exist.
- (2) External optical cavity. Very attractive solution, but needs very high tolerances and mirror quality. Serious R&D is required.
- (3) Free electron laser. Is attractive due to variable wave length. High electron to photon energy conversion efficiency required is a problem.

5 Experimentation issues

Backgrounds at the TESLA photon collider were discussed in the TESLA Conceptual design [3]. More simulations are necessary with detailed geometry and material. Here we consider only two geometric questions connected with optics inside the detector.

Main background in the vertex detector are e^+e^- pairs produced in e^+e^- , γe and $\gamma\gamma$ interactions. It is very similar to that in e^+e^- collisions and may differ only in numbers. The shape of the zone occupied by the electrons kicked by the opposing beam is described by the formula [50],[13]

$$r_{max}^2 \simeq \frac{25Ne}{\sigma_z B} z \sim 0.12 \frac{N}{10^{10}} \frac{z[\text{cm}]}{\sigma_z[\text{mm}] B[\text{T}]}, [\text{cm}^2] \quad (12)$$

where r is the radius of the envelope at a distance z from the IP, B is longitudinal detector field. For example, for TESLA ($N = 2 \times 10^{10}$, $\sigma_z = 0.3$ mm, $B = 3$ T) $r[\text{cm}] = 0.52\sqrt{z[\text{cm}]}$.

So, from the background consideration it follows than the vertex detector with a radius 2 cm can have the length about ± 15 cm and a clear angle for the laser beams is ± 130 mrad.

As it was shown (see eq.5) the r.m.s. divergence of the the laser beam at the conversion point $\sigma_{x'} = 0.0155$; 2.5σ will be sufficient. As we consider the optics situated outside the electron beams, the required clear angle is $\pm 2 \times 2.5 \times 0.0155 = \pm 78$ mrad. As we see the laser beams have enough space inside the vertex detector.

Together all the optics inside the detector covers the angle about 120–140 mrad (fig.11). However, it does not mean that this region is lost for the experiment. The thickness of mirrors will be of the order of $1 X_0$, and that will not affect too much the performance of the calorimeter placed behind the mirrors.

6 Conclusion

Due to the potential decrease of the horizontal beam emittance in the TESLA damping ring the luminosity in $\gamma\gamma$ collisions (in the high energy peak) can reach about 40% of e^+e^- luminosity. Since cross sections in $\gamma\gamma$ collisions are typically higher by one order of magnitude than those in e^+e^- collisions and because $\gamma\gamma$, γe collisions give access to higher masses of some particles, the photon collider now has very serious physics motivation.

The key problem for photon colliders is the powerful laser system. There are several possible laser-optics schemes for photon collider at TESLA. One of them has no visible problems and, it seems, can be build now.

Acknowledgments

I would like to thank K. Van Bibber, E. Boos, R. Brinkmann, W. Decking, A. Gamp, M. Galynskii, J. Gronberg, A. De Roeck, I.F. Ginzburg, K. Hagiwara, R. Heuer, C. Heusch, V. Ilyin, G. Jikia, M. Krawczyk, J. Kwiecinski, D. Miller, M. Perry, S. Soldner-Rembold, T. Rizzo, W. Sandner, S. Schreiber, V. Serbo, A. Skrinsky, T. Takahashi, D. Trines, A. Wagner, I. Will, N. Walker, I. Watanabe, M. Yurkov, K. Yokoya, P. Zerwas and all participants of the GG2000 workshop for useful discussions and support of photon colliders.

References

- [1] *Zeroth-Order Design Report for the Next Linear Collider* LBNL-PUB-5424, SLAC Report 474, May 1996.
- [2] *JLC Design Study*, KEK-REP-97-1, April 1997; I. Watanabe et. al., KEK Report 97-17.
- [3] *Conceptual Design of a 500 GeV Electron Positron Linear Collider with Integrated X-Ray Laser Facility* DESY 97-048, ECFA-97-182.
- [4] J.P. Delahaye et al., *Acta Phys. Polon. B30:2029-2039*, 1999; R. Bossart et al. CERN-PS-99-005-LP, Apr 1999. 4pp.
- [5] I. Ginzburg, G. Kotkin, V. Serbo, V. Telnov, *Pizma ZhETF*, **34** (1981) 514; *JETP Lett.* **34** (1982) 491.
- [6] I. Ginzburg, G. Kotkin, V. Serbo, V. Telnov, *Nucl. Instr. and Meth.* **205** (1983) 47 (Prepr. INP 81-102, Novosibirsk, 1991).
- [7] I. Ginzburg, G. Kotkin, S. Panfil, V. Serbo, V. Telnov, *Nucl. Instr. and Meth.* **219**(1984)5 (Prepr. INP 82-160, Novosibirsk, 1982).
- [8] V. Telnov, *Nucl. Instr. and Meth.* **A 294** (1990) 72.
- [9] V. Telnov, *Nucl. Instr. Meth.* **A 355** (1995) 3.
- [10] *Proc. of Workshop on $\gamma\gamma$ Colliders*, Berkeley CA, USA, 1994, *Nucl. Instr. & Meth.* **A 355** (1995).
- [11] V. Telnov, Goals of the Workshop GG2000, these proceedings.

- [12] T. Takahashi, these proceedings.
- [13] R. Brinkmann et al., *Nucl. Instr. and Meth. A* **406** (1998) 13.
- [14] A. Grutu, talk at ICHEP2000, Osaka, Japan, 27 July – 2 August, 2000.
- [15] L.B. Okun, *Leptons and Quarks*, North-Holand, Amsterdam, 1982.
- [16] V.Telnov, *Int. J. Mod. Phys. A* **13** (1998) 2399, e-print:hep-ex/9802003.
- [17] M. Battaglia, HU-P-264, Apr 1999, To be published in the proceedings of 4th International Workshop on Linear Colliders (LCWS 99), Sitges, Barcelona, Spain, 28 Apr - 5 May 1999, e-print: hep-ph/9910271.
- [18] G. Jikia, S. Soldner-Rembold, Proceedings of 4th International Workshop on Linear Colliders (LCWS 99), Sitges, Barcelona, Spain, 28 Apr - 5 May 1999. e-print: hep-ph/9910366.
- [19] M. Melles, W.J. Stirling, V.A. Khoze, *Phys.Rev. D* **61** (2000) 054015, e-print: hep-ph/9907238.
- [20] S. Soldner-Rembold, G. Jikia, these proceedings.
- [21] I. Ginzburg, M. Krawczyk, Proceedings of 4th International Workshop on Linear Colliders (LCWS 99), Sitges, Barcelona, Spain, 28 Apr - 5 May 1999, hep-ph/9909455 and these proceedings.
- [22] E. Accomando et al., *Phys. Rep.* **299** (1998) 1.
- [23] M.M. Muhlleitner, this proceedings.
- [24] V. Telnov, Proc. of the International Conference on the Structure and Interactions of the Photon (Photon 99), Freiburg, Germany, 23-27 May 1999, *Nucl. Phys. Proc. Suppl. B* **82** (2000) 359, e-print: hep-ex/9908005.
- [25] I.F. Ginzburg, these proceedings.
- [26] N. Arkani-Hamed, S. Dimopoulos, G. Dvali. SLAC-PUB-7769, March 1998, *Phys. Lett. B* **429** (1998) 263, hep-ph/9803315.
- [27] Thomas Rizzo, *Proceedings of 4th International Workshop on Linear Colliders (LCWS 99)*, Sitges, Barcelona, Spain, 28 Apr - 5 May 1999, SLAC-PUB-8204, e-Print: hep-ph/9907401, also these proceedings.
- [28] M. Ferrario, these proceedings.
- [29] W. Decking, these proceedings.
- [30] K. Hirata, K. Oide, B. Zotter, *Phys. Lett. B* **224** (1989) 437.
- [31] N. Walker, these proceedings.
- [32] P. Raimondi, A. Seryi, SLAC-PUB-8460, May 2000. Submitted to *Phys. Rev. Lett.*
- [33] A. Seryi, private communication.

- [34] R. Brinkmann, TESLA 99-15, Sep. 1999, To be published in the proceedings of 4th International Workshop on Linear Colliders (LCWS 99), Sitges, Barcelona, Spain, 28 Apr - 5 May 1999.
- [35] M. Galynskii, E. Kuraev, M. Levchuk, V. Telnov, these proceedings.
- [36] J.F. Gunion and J.G. Kelly, Phys.Lett.**B333** (1994) 110.
- [37] M. Kramer, J. Kuhn, M. Strong and P. Zerwas, Z.Phys. C64 (1994) 21.
- [38] P. Chen, V. Telnov, *Phys. Rev. Lett.*, **63** (1989) 1796.
- [39] V.Telnov, SLAC-PUB-7337, *Phys.Rev.Lett.*, **78** (1997) 4757, erratum *ibid* 80 (1998) 2747, e-print: hep-ex/9610008.
- [40] V.Telnov, *Proc. Advanced ICFA Workshop on Quantum aspects of beam physics*, Monterey, USA, 4-9 Jan. 1998, World Scientific, p.173, e-print: hep-ex/9805002.
- [41] V.Telnov, Proc. of Intern. Symp. on New Visions in Laser-Beam Interactions, October 11-15, 1999, Tokyo, Metropolitan University Tokyo, Japan. Nucl.Instr. and Meth. A 450 (2000) 63, hep-ex/0001029.
- [42] I. Will, T. Quast, H. Redlin and W. Sandner, these proceedings.
- [43] J. Andruszkow et al., DESY-00-066, May 2000, e-print: physics/0006010.
- [44] E.L. Saldin, E.A. Schneidmiller and M.V. Yurkov, these proceedings.
- [45] V.G. Serbo, these proceedings.
- [46] V.B. Berestetskii, E.M. Lifshitz and L.P. Pitaevskii, *Quantum electrodynamics* (Pergamon Press, Oxford, 1982).
- [47] W. Koechner, *Solid State Laser Engineering*, Springer-Verlag.
- [48] J. Gronberg, these proceedings.
- [49] S.A. Payne, C. Bibeau, C.D. Marshall, H.T. Powell, UCRL-JC-119366, preprint LLNL, Dec.1998.
- [50] M. Battaglia, A. Andreazza, M. Caccia, V.Telnov, HIP-1997-522-exp, 1997; *Proc. of 2nd Workshop on Backgrounds at Machine Detector Interface*, Honolulu, HI, 21-22 Mar 1997.